Journal of Atmospheric and Terrestrial Physics, Vol. 48, Nos. 11–12, pp. 1269–1278, 1986.
Printed in Great Britain.

0021–9169/86 $3.00+ .00
Pergamon Journals Ltd.

High resolution turbulence observations in the middle and lower atmosphere by the MU radar with fast beam steerability: preliminary results

SHOICHIRO FUKAO*

Department of Electrical Engineering, Kyoto University, Yoshida, Kyoto 606, Japan

TORU SATO, TOSHITAKA TSUDA, MAMORU YAMAMOTO and SUSUMU KATO

Radio Atmospheric Science Center, Kyoto University, Uji, Kyoto 611, Japan

(*Received for publication* 10 *March* 1986)

Abstract—Refractive index fluctuations or turbulence in the mesosphere, stratosphere and troposphere are observed with the aid of the fast beam steerability of the MU (middle and upper atmosphere) radar which operates at 46.5 MHz with 1 MW peak radiation power and 8330 m^2 antenna aperture. Morphology of the mesospheric and stratospheric turbulence is studied by making use of the high altitude and time resolutions. Sixteen beam observations based on the fast beam steerability reveal advection properties and spatial variability of echoing regions in the troposphere. These results demonstrate new possibilities for this system in the investigation of three dimensional structures of turbulence.

1. INTRODUCTION

MST (mesosphere–stratosphere–troposphere) radars are sensitive, high power VHF/UHF Doppler radars that can detect regions of refractive index fluctuations or turbulence in the middle and lower atmosphere (see BALSLEY and GAGE, 1980, 1982; GAGE and BALSLEY, 1984; GREEN *et al.*, 1979; HARPER and GORDON, 1980; LARSEN and RÖTTGER, 1982; RÖTTGER, 1984, for reviews). This type of equipment can enable us to establish the temporal and spatial morphology of turbulence in this height range, which are important parameters in determining the role played by turbulence in the vertical transport of tracers and contaminants (e.g. WOODMAN, 1980b).

The turbulence echoes are not distributed uniformly with altitude, but rather occur intermittently in both height and time. Strong echoes, however, may persist from given height ranges for periods of the order of tens of minutes to hours.

RÖTTGER *et al.* (1979) and CZECHOWSKY *et al.* (1979) identified different types of turbulence structures in the mesosphere, i.e. blobs or sheets having a thickness of 300 m or less and layers of the order of 1 km thick, using the fixed vertical beam of the SOUSY radar. High resolution MST radar studies of the stratosphere and troposphere also provided evidence of turbulence layers as thin as the available altitude resolutions, despite the variety of frequencies of the systems employed. These results were all obtained by employing the fixed beams of the Arecibo 430 MHz radar (WOODMAN, 1980a,b), the SOUSY 54 MHz radar (RÖTTGER, 1980; RASTOGI and RÖTTGER, 1982) and the Millstone Hill *L*-band radar (WAND et al., 1983). A VAD (velocity–azimuth display) observation with the aid of a fully steerable dish at Chatanika (operating frequency 1290 MHz) resulted in the detection of an intense azimuthal variation of echo power, which suggested a turbulence in the shape of a parallel roll oriented horizontally (BALSLEY and GAGE, 1980). However, more observations apparently need to be performed to map the echo power horizontally with a fast steerable antenna and to determine the three dimensional structures of turbulence.

Here we describe a series of preliminary measurements conducted recently using the fast beam steerability of the MU radar, which is located at Shigaraki (34.85°N, 136.10°E), about 50 km southeast of Kyoto, Japan. The observed echoing regions would generally be classified as clear air turbulence, but some of them, particularly those observed in the troposphere, may presumably arise from cloud-enhanced refractive index fluctuations. These results, which are

*Present address: Radio Atmospheric Science Center, Kyoto University.

an outgrowth of previously reported standard observations using either a single fixed beam or three beams (e.g. KATO *et al.*, 1984; FUKAO *et al.*, 1985c,d; TSUDA *et al.*, 1985; SATO *et al.*, 1985), illustrate new possibilities for the investigation of three dimensional structures of turbulence in more detail.

2. THE MU RADAR SYSTEM

The MU radar operates on 46.5 MHz and uses an active phased array system (FUKAO *et al.*, 1980). It is composed of 475 Yagi antennas and an equivalent number of solid state power amplifiers [transmitter–receiver (TR) modules] (KATO *et al.*, 1984; FUKAO *et al.*, 1985a). Each Yagi antenna is driven by a TR module with peak output power of 2.4 kW. The nominal peak and average radiation powers of the whole system are 1000 and 50 kW, respectively. This system makes it possible to steer the antenna beam up to 30° from the zenith in each interpulse period. The basic parameters of the MU radar are given in Table 1. Further details of the system have been given by KATO *et al.* (1984) and FUKAO *et al.* (1985a,b).

3. FOUR BEAM MESOSPHERE OBSERVATION

The mesosphere observation presented here was conducted during a 7 h period on 7 February 1985.

Table 1. Basic parameters of the MU radar

Radar system:	Monostatic pulse radar; active phased array system
Operational frequency:	46.5 MHz
Antenna:	Circular array of 475 crossed Yagi antennas
Aperture:	8330 m^2 (103 m in diameter)
Beam width:	3.6° (half power for full array)
Steerability:	Steering is completed in each IPP
Beam directions:	1657; 0–30° off-zenith angle
Transmitter:	475 solid-state amplifiers (TR-modules; each with output power of 2.4 kW peak and 120 W average)
Peak power:	1 MW (max)
Average power:	50 kW (duty ratio 5%) (max)
Bandwidth:	1.65 MHz (max) (pulse width: 1–512 μs variable)
IPP:	400 μs–65 ms (variable)
Receiver:	
Dynamic range:	70 dB
A/D converter:	12 bits × 8 channels
Pulse compression:	Binary phase-coding up to 32 elements (Barker and complementary codes presently in use)

The beam was steered during each interpulse period (IPP) of 1300 μs sequentially to four different directions: 5° from the zenith to the north, east, south and west, respectively. The transmitted pulse was phase modulated by a 16 element complementary code with 4 μs baud length, corresponding to a height resolution of 600 m.

The baseband signal from each beam was sampled at 64 points spaced in the region from 60 to 98.1 km at 600 m intervals. Coherent integration was performed 30 times in each beam direction. Then, 128 point complex fast Fourier transforms (FFT's) were calculated in real time to obtain Doppler velocity spectra for each 20 s period. The resulting power spectra were averaged for approximately 200 s before being written on magnetic tape.

Figure 1 shows a time–height contour of the mesospheric echo power obtained in the westward beam, where three echoing layers of fairly intense turbulence are observed. The lower two layers remain at almost the same heights for more than several hours, while the top thinner layer shows a clear descending motion with time. These layers are also observed in the other three beams at the same heights and with the same shape as in the westward beam. No direct correspondence was found between the echo power variation and wind fluctuations.

The three layers, if they are assumed to have a very long persistency, are spread quite widely over a distance of more than 400–800 km, considering the horizontal wind velocity of about 20–40 m s^{-1} observed during this period. However, from this observation the possibility that they are continuously generated in the neighbourhood of the radar cannot be denied. On the other hand, small structures embedded in each layer which have a signal-to-noise ratio of more than 2 dB were not always observed in the other three beams, suggesting that the small scale intense turbulence has a horizontal dimension of less than 12 km.

The discrete intense echoes above approximately 80 km are generated by meteor trails. On average the MU radar receives more than 4000 meteor echoes a day, which are utilized to infer horizontal wind velocities in this height range (TSUDA *et al.*, 1985), as has been done at Poker Flat by AVERY *et al.* (1983).

4. THREE BEAM STRATOSPHERE–TROPOSPHERE OBSERVATION

The present stratosphere–troposphere data was obtained over a 32 h period on 9–10 May 1985. The beam was steered in the standard mode or every IPP

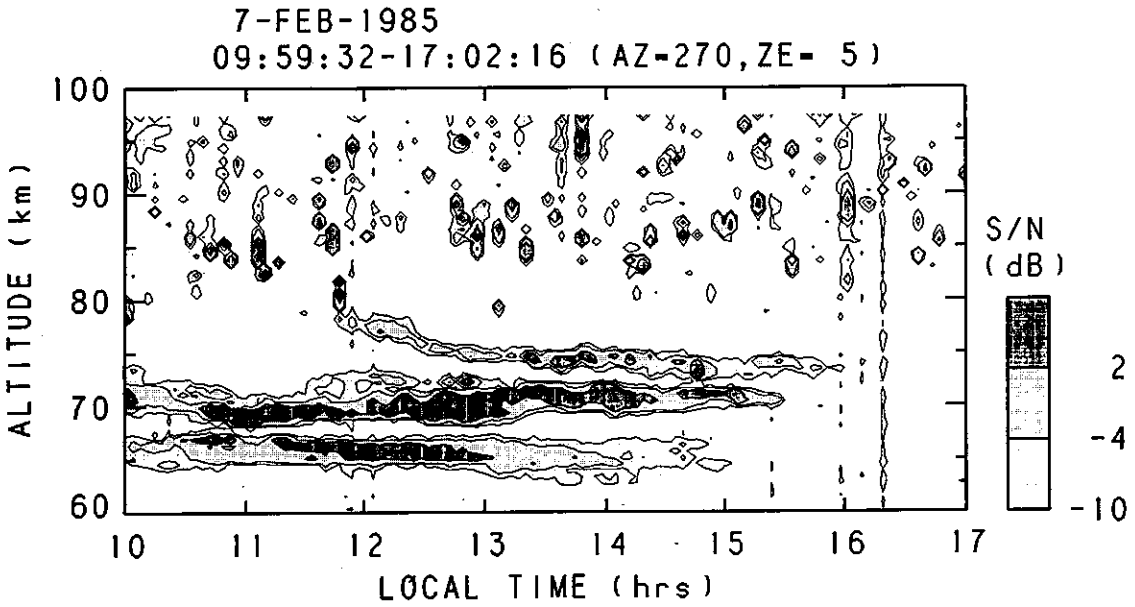

Fig. 1. Time–height contour of the mesospheric echo power observed in the westward beam on 7 February 1985. The echo power over the noise level is given at 6 dB intervals, as shown on the scale on the right-hand side.

to three directions: the zenith and 10° away from the zenith to the north and east. The transmit pulse scheme was the same as for the mesosphere observation mentioned above, except for the baud length, which was 1 μs with a corresponding height resolution of 150 m. The IPP was 400 μs. One hundred and twenty-eight heights in the range of 5.4–24.5 km were sampled at 150 m intervals in each direction. The number of coherent integrations performed was 64. The time resolution was approximately 150 s.

The top diagram in Fig. 2 shows a time-height section of the echo power obtained in the zenith direction. Basic scattering properties detected previously by other high resolution MST radar observations (e.g. RÖTTGER and SCHMIDT, 1979; WOODMAN *et al.*, 1980a; SATO and WOODMAN, 1982; SATO *et al.*, 1985) are also observable in this diagram. In the troposphere intense echoing regions exhibit large temporal and spatial variability, often showing a clear downward motion. On the other hand, echoing regions due to turbulence in the stratosphere are characterized by separate layer structures which are much thinner and more stable than the echoing regions in the troposphere, if they are assumed to have a very long persistency. The thickness of these structures seems to be comparable to, or even smaller than, the height resolution of 150 m, because the echo power above and below the layer is usually much lower than at the peak height. The persistency of these thin layers is probably related to atmospheric stability, as discussed by GAGE and GREEN (1978). The potential temperature gradient calculated from the routine rawinsonde observations at Shionomisaki, approximately 150 km south of the MU radar, exceeds 10–15K km^{-1} in the stratosphere.

The heavy crosses are the tropopause heights determined from the routine rawinsondes launched at the standard 12 h intervals. The meteorological tropopause at Shionomisaki is not always associated with strong echoing layers at Shigaraki, as is illustrated at 9 LT (Japan Standard Time) on 9 May 1985. This result contrasts with observations at higher latitudes, which generally show excellent agreement (e.g. GAGE and GREEN, 1978; RÖTTGER, 1980). The disagreement is observed by the MU radar, as well as by the Chung-Li VHF radar, which are both located at lower latitudes where the tropopause may have different characteristics with respect to VHF radar reflectivities compared with those at higher latitudes (RÖTTGER, 1985).

The bottom diagram in Fig. 2 shows the ratio of the echo power in the zenith to that in the 10° oblique direction. The ratio is higher where the layer structure is observed, even in the troposphere, as on 9 May 1985. The scattering seems to be isotropic in the troposphere on 10 May, though a fairly intense echo is

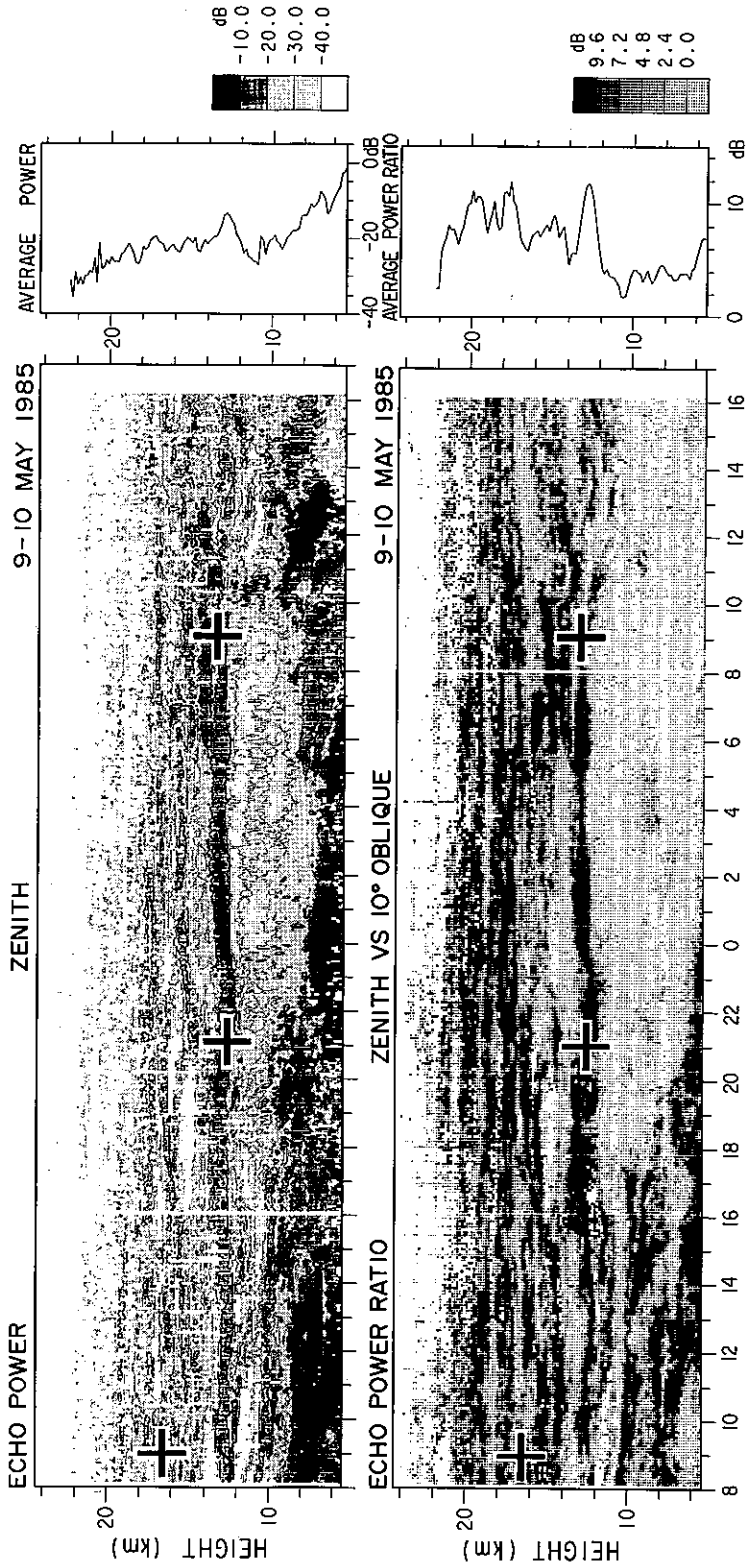

Fig. 2. (Top) Time–height contour of echo power observed in the zenith direction in the height range 5.4–24.5 km on 9–10 May 1985. The tropopause heights determined by routine meteorological rawinsondes are given by heavy crosses. The echo power is in an arbitrary unit and contours are drawn at 10 dB intervals, as shown by the contour scale on the right-hand side. (Bottom) Echo power ratio of the zenith to the 10° oblique direction. The ratio is given in dB, as shown by the contour scale.

obtained there. This manner of presentation seems to be useful for identifying stable atmospheric regions (GAGE and GREEN, 1979). The mean echo power ratio shown on the right-hand side exceeds 10 near the tropopause and at several heights above it. The general tendency for stronger aspect sensitivity to be associated with thinner and more persistent turbulence layers is explained by the partial reflection mechanism (e.g. RÖTTGER and LIU, 1978). One of the several heights with strong aspect sensitivity corresponds to the tropopause, but the tropopause is not necessarily located at the most aspect sensitive height. Detailed examination of the aspect sensitivity of individual turbulence layers should prove to be very interesting.

5. SIXTEEN BEAM VAD OBSERVATION OF TROPOSPHERE

A VAD technique (e.g. BALSLEY *et al.*, 1977; FARLEY *et al.*, 1979), which was first applied to the MU radar by WAKASUGI *et al.* (1985, 1986), was employed for investigation of azimuthal variation of scattering in the troposphere. As shown in Fig. 3, the antenna beam was sequentially steered to 16 oblique directions with a zenith angle of 15°. The diameter of the VAD circle was 4–5 km at an altitude of 8–9 km. The beam direction was switched every interpulse period (400 μs) and the echo from each beam was sampled at 64 heights in the range 5.2–14.3 km at 150 m intervals. After coherently integrating over 8 beam steering periods, Doppler velocity spectra were estimated from 128 point real time FFT's and then averaged for approximately 100 s. A 16 element complementary code with baud length of 1 μs was again used.

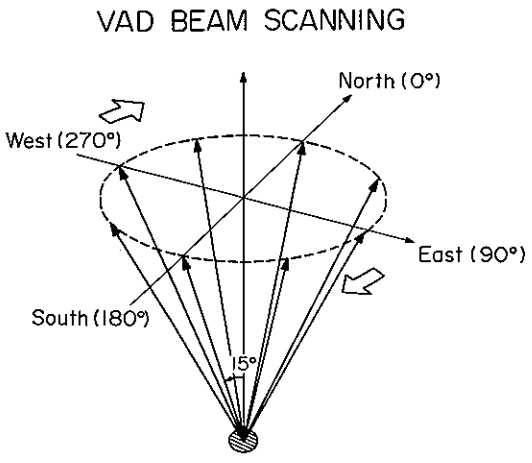

Fig. 3. A schematic diagram of VAD beam steering. The antenna beam is steered in 16 directions with zenith angle of 15° and azimuthal angles of 0° (north), 20°, 45°, 65°, 90° (east), 110°, 135°, 155°, 180° (south), 200°, 225°, 245°, 270° (west), 290°, 315° and 335°, respectively.

The observation was conducted over a 48 h period on 28–30 June 1984. It should be noted that plots of radial velocity as a function of azimuth (VAD) generally show very clear sinusoidal variations along this comparably small VAD circle. Figure 4(a) shows a time–height contour of echo power observed in the northward beam. The echo power profile in the same beam direction averaged over the 48 h period is given in Fig. 4(b). Although the time–height contour varies considerably in the 16 directions, the mean echo power profile changes very little within the VAD circle of several kilometres in diameter. The decrease of echo power profile in the troposphere is 4 dB km^{-1} with normalization of the range squared. This value is representative of this height range, although the day-to-day variability is very large.

Figure 5 is a time–azimuth diagram of echo power obtained in a 1 h period at five adjacent heights. There appear to be two echo regions in this period, which are presumably due to enhanced humidity in high clouds passing by. Both regions show a systematic time lag in detecting echoes in the individual beam directions, or an S-shaped echo contour. Regardless of the small structures observed in each region, both regions first appear in the VAD circle at an azimuth angle of near 270° (west) and disappear in the opposite direction (east). Since the horizontal wind at this height range was almost westerly (eastward) during this period, the S-shaped echo contour illustrates that the echoing regions are advected with the mean wind. Considering the zonal wind velocity observed during this period, and assuming the persistency of the echoing regions, the horizontal dimensions in the east–west direction are roughly estimated to be 15 and 30 km for the first and second regions, respectively. The half-power thickness of these regions is less than 500 m, of the order of one fiftieth of the horizontal scale.

This particular observation, however, is not well suited for tracking the motion of each echoing region [in which BALSLEY and PETERSON (1981) succeeded, though not perfectly], since the dimensions of the echo region observed are apparently much larger than the diameter of the VAD circle or approximately 5 km in the height range considered. A more definitive observation needs to be conducted in a clear sky to determine if the clear air turbulence moves at identically the same speed as the ambient atmosphere.

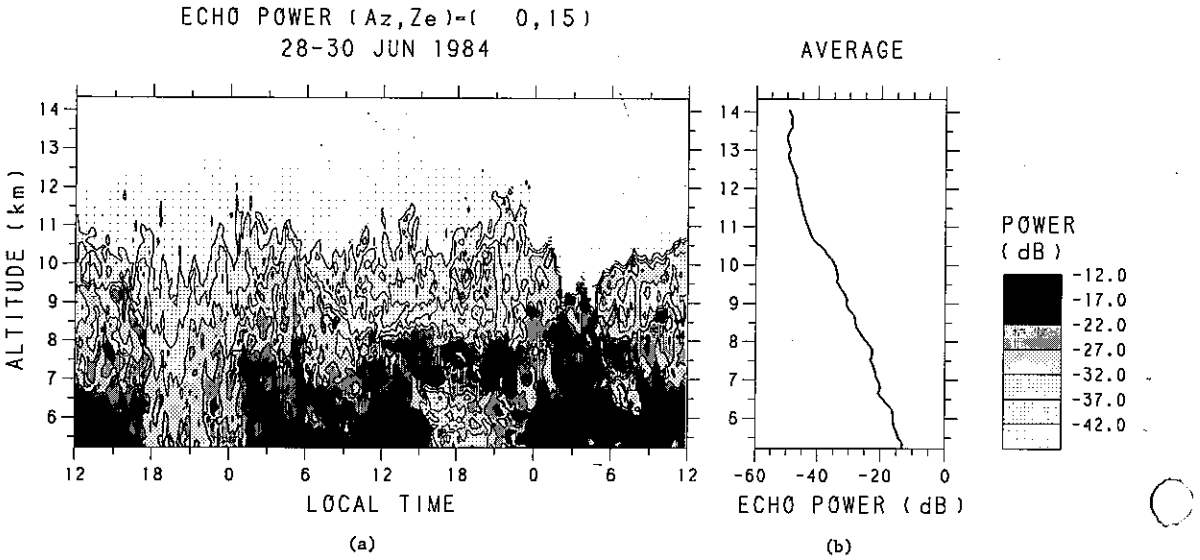

Fig. 4. (a) Time–height contour of the echo power observed in the direction tilted 15° from the zenith toward the north from 12 LT on 28 June to 12 LT on 30 July 1984. The echo power is in an arbitrary unit. The contour scale is given on the right-hand side of the figure. (b) The echo power profile in the same direction as (a) averaged over the 2 day period.

6. SIXTEEN BEAM GRID STEERING IN TROPOSPHERE OBSERVATION

In order to investigate the small scale horizontal structure of turbulence the antenna beam was directed to the 16 grid points shown in Fig. 6. The center of the square is the zenith and the beam positions are given by asterisks with a pair of numbers representing the azimuthal and off-zenith angles of the beams. The outermost beams are 10° from the zenith. The side of the square is approximately 3 km in length at a height of 10 km.

The observation was conducted on 18 May 1985. The beam was switched every interpulse period (400 μs) and the echo from each beam was sampled at 64 ranges at 300 m intervals. The samples were coherently integrated 8 times in each direction. Doppler spectra were estimated from 128 point real-time FFT's and then averaged for 1 min before being written on magnetic tape. An uncoded pulse 2 μs in width with a corresponding range resolution of 300 m was used.

Figure 7 shows the spatial variation of echo power obtained in a 1 min period at three different heights. The echo contours are given by a two dimensional spline approximation by which contours are extrapolated to the places where no beam is directed. At the lower two heights the iso-power contour is constructed in a concentric configuration, showing a two dimensional aspect sensitivity of the scattering. The echo power decreases by 5–10 dB at the 8° off-zenith directions compared with that at the zenith in both the stratosphere and the troposphere during the period of this observation (cf. fig. 3 of SATO *et al.*, 1985). This result suggests that echoing regions with a horizontal dimension much wider than the illuminated region of the beam are located over the radar or that in the case when a single echoing region does not exist the anisotropic or diffuse partial reflection is considered to be predominant. It is considered that the edge of an echoing region is detected at the height shown in the top diagram. However, the horizontal pattern shown is also describable by a focusing effect due to reflecting layers undulated by gravity waves (e.g. GAGE *et al.*, 1981). Anyway, temporal development of the echo contours would be interesting and time series of subsequent contour diagrams will be shown elsewhere.

The wind vector is estimated at four points at the same height using a set of three beams located at the apices of the triangles shown in Fig. 8. An arithmetic mean is then arrived at to give the mean wind field at the zenith point, and the difference of the wind velocity at each point from the mean wind field is calculated to infer the non-uniformity of the wind field inside the square.

Figure 9 shows histograms of the difference for the eastward, northward and upward velocity, respec-

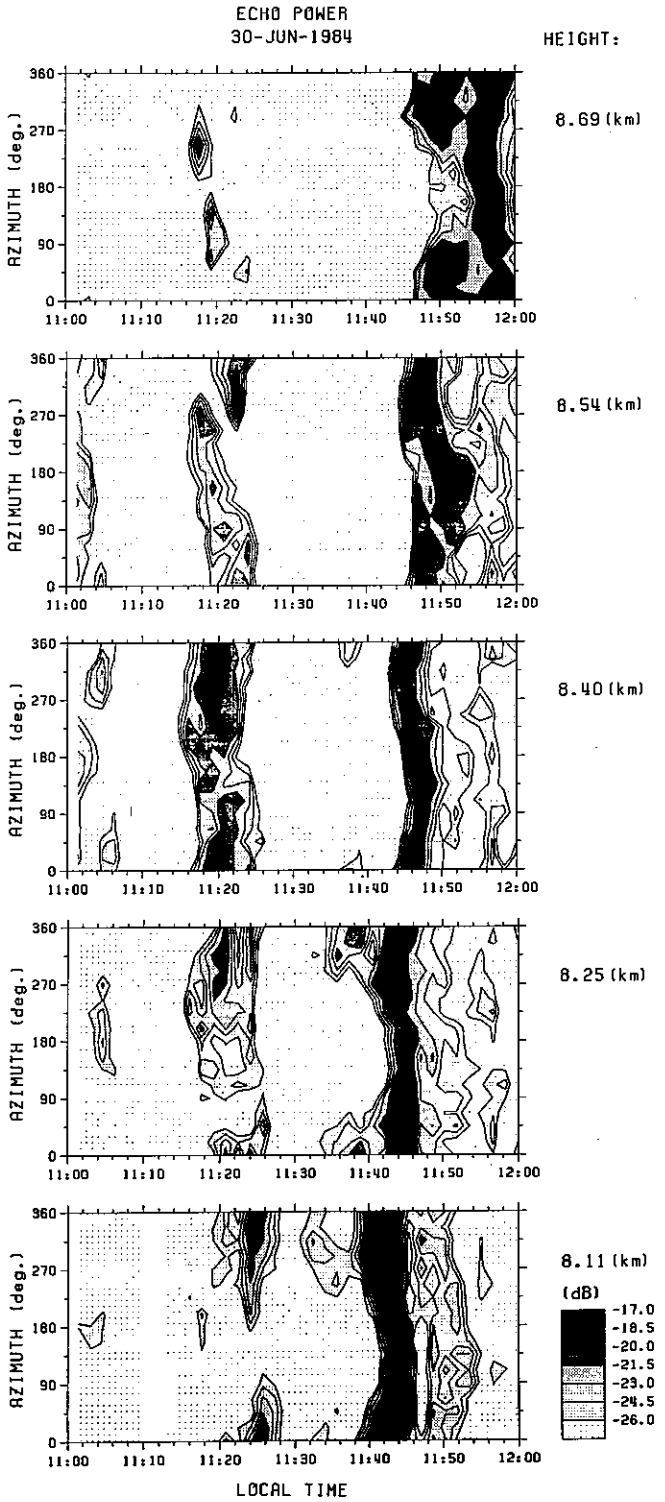

Fig. 5. Time–azimuth contour of echo power obtained in the 1 h period 11–12 LT on 30 June 1984 at five adjacent heights separated by 150 m. The contour scale is shown on the bottom right.

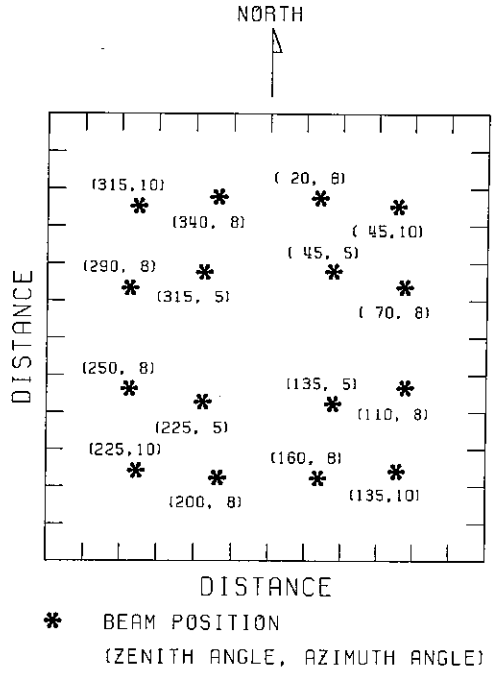

Fig. 6. Beam positions for 16 grid point steering. The center is the zenith direction. The beam positions are given by asterisks with a pair of numbers showing the beams' azimuthal and zenith angles in degrees.

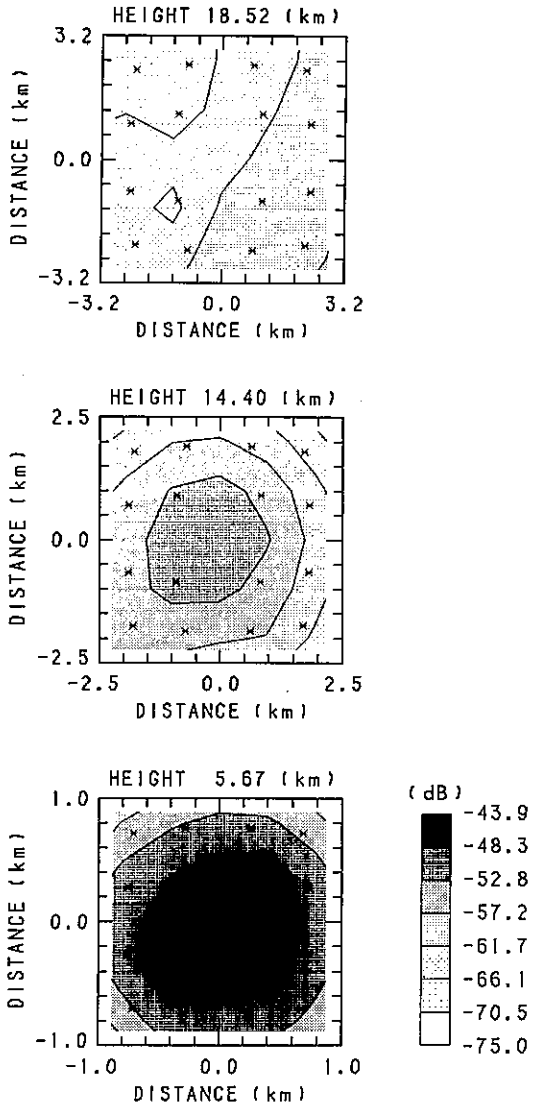

Fig. 7. Spatial variation of echo power obtained in a 1 min period at three different heights, 5.67, 14.4 and 18.52 km, respectively. The asterisks represent the beam positions depicted in Fig. 6. The contour scale is given on the right-hand side.

tively. Data was averaged for a 2 h period over the height range 5.61–10.04 km. The mean eastward, northward and upward wind velocities are 14.68, −3.35 and 0.04 m s^{-1}, respectively. The apparent variances of approximately 1 m s^{-1} for the horizontal components are relatively small compared with the mean wind velocities. However, a fairly large spatial variation is observed in the vertical direction. The value is ten times larger than the mean vertical velocity.

This result shows caution when using the conventional three beam method to discuss short term fluctuation of the horizontal wind component, since it may be dominated by spatial fluctuation of the vertical component. In this sense, the variance of the horizontal wind component obtained here may contain a larger error than that of the vertical component.

For the MU radar the wind velocity is estimated by fitting a Gaussian function to each observed spectrum (FUKAO *et al.*, 1985b). The solid smooth lines in Fig. 9 show the theoretical distribution of error due to statistical fluctuation when wind velocity is determined by this fitting procedure. The theoretical distribution is obtained by performing the following computer simulation of the actual fitting procedure.

Since each point of the echo power spectrum obtained by the periodgram method employed here can safely be regarded as obeying the χ^2 distribution of freedom 2 as far as the echo is produced by a random process, it has a r.m.s. (root mean square) fluctuation equal to the magnitude of its spectral density, regardless of the physical processes involved. This fluctuation is suppressed only through the incoherent integration. Therefore, theoretical spectra used in the

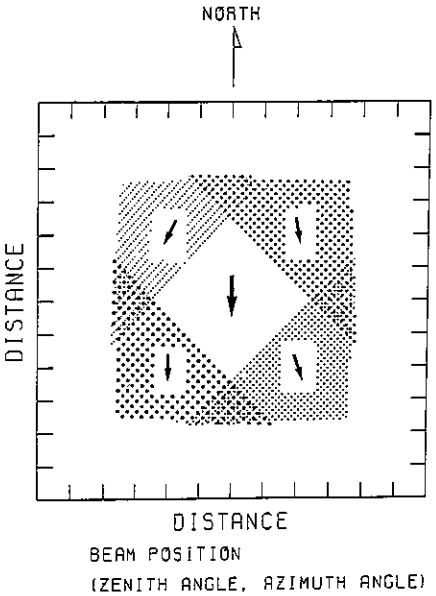

Fig. 8. The thin arrows schematically show wind vectors determined by using a set of three beams located at the apices of the triangles shown by different shadings. The thick arrow at the center (the zenith) is the mean wind field determined by the four wind vectors.

simulation were generated to produce the same amount of random fluctuation as the observed ones. Spectral broadening effects, such as beam broadening due to the horizontal wind or broadening due to wave motions, were inclusively taken into consideration by adjusting the theoretical spectral width to the observed value. In order to obtain a statistical mean, simulation was repeated 100 times for the same case with different random series. It is to be noted that the estimated error does not include any contribution from wind fluctuations on spatial scales larger than the beam width.

The observed variance, which is regarded as principally due to small scale wind fluctuations, is approximately 2.5 times larger than the estimated error and is physically significant. It will be interesting to investigate small scale wind flucutations in further detail using this technique.

7. CONCLUDING REMARKS

Fine resolution radar observations of refractive index fluctuations or turbulence in the mesosphere, stratosphere and troposphere were carried out with the aid of the fast beam steerability of the MU radar. Preliminary results show that the MU radar is living up to the high standard of performance specified by the design. Sensitive MST radars equipped with fast beam steerability, like the MU radar, are expected to open up new possibilities for the investigation of both turbulence structures and the ambient wind fields with which they are in close relationship.

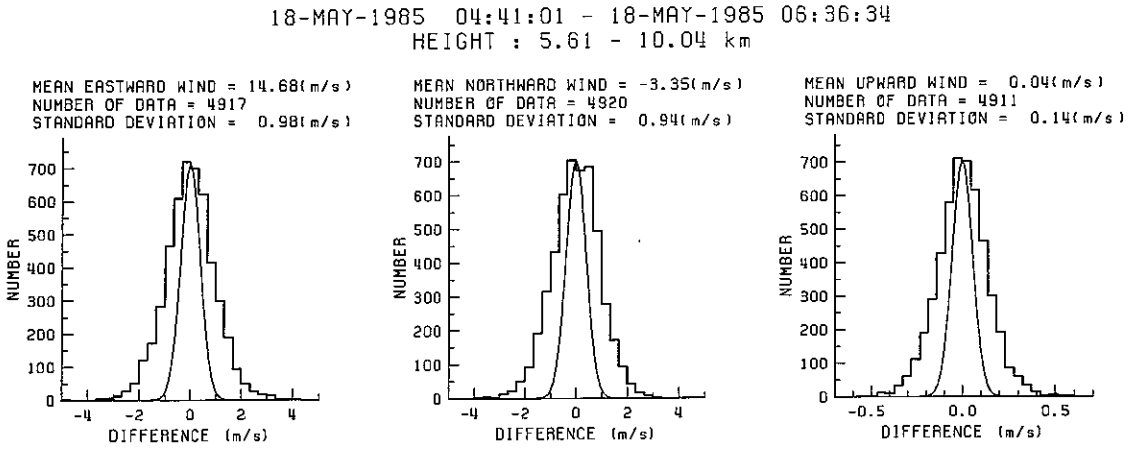

Fig. 9. Histograms showing the difference in wind velocity at each of the four points from the mean wind. (Left) eastward, (center) northward and (right) upward component, respectively. Data was averaged over approximately a 2 h period on 18 May 1985 for the height range 5.61–10.04 km. The smooth solid lines indicate the theoretically estimated error, which is caused by statistical fluctuation when wind velocity is determined by fitting a Gaussian function to each observed spectrum.

Acknowledgements—The authors wish to thank the referees for their constructive comments and suggestions. They are grateful also to Messrs H. MATSUMOTO and A. ITO of the Department of Electrical Engineering, Kyoto University, for their assistance in the data analysis. The MU radar is operated by the Radio Atmospheric Science Center of Kyoto University.

REFERENCES

AVERY S. K., RIDDLE A. C. and BALSLEY B. B.	1983	*Radio Sci.* **18,** 1021.
BALSLEY B. B. and GAGE K. S.	1980	*Pure appl. Geophys.* **118,** 452.
BALSLEY B. B. and GAGE K. S.	1982	*Bull. Am. met. Soc.* **63,** 1009.
BALSLEY B. B. and PETERSON V. L.	1981	*J. appl. Met.* **20,** 266.
BALSLEY B. B., CIANOS N., FARLEY D. T. and BARON M. J.	1977	*J. appl. Met.* **16,** 1235.
CZECHOWSKY P., RÜSTER R. and SCHMIDT G.	1979	*Geophys. Res. Lett.* **6,** 459.
FARLEY D. T., BALSLEY B. B., SWARTZ W. E. and LAHOZ C.	1979	*J. appl. Met.* **18,** 227.
FUKAO S., KATO S., ASO T., SASADA M. and MAKIHIRA T.	1980	*Radio Sci.* **15,** 225.
FUKAO S., SATO T., TSUDA T., KATO S., WAKASUGI K. and MAKIHIRA T.	1985a	*Radio Sci.* **20,** 1155.
FUKAO S., TSUDA T., SATO T., KATO S., WAKASUGI K. and MAKIHIRA T.	1985b	*Radio Sci.* **20,** 1169.
FUKAO S., WAKASUGI K., SATO T., MORIMOTO S., TSUDA T., HIROTA I., KIMURA I. and KATO S.	1985c	*Nature* **316,** 712.
FUKAO S., WAKASUGI K., SATO T., TSUDA T., KIMURA I., TAKEUCHI N., MATSUO M. and KATO S.	1985d	*Radio Sci.* **20,** 622.
GAGE K. S. and BALSLEY B. B.	1984	*J. atmos. terr. Phys.* **46,** 739.
GAGE K. S. and GREEN J. L.	1978	*Radio Sci.* **13,** 991.
GAGE K. S. and GREEN J. L.	1979	*Science* **203,** 1238.
GAGE K. S., CARTER D. A. and ECKLUND W. L.	1981	*Geophys. Res. Lett.* **8,** 599.
GREEN J. L., GAGE K. S. and VAN ZANDT T. E.	1979	*IEEE Trans. Geosci. Electron.* **GE-17,** 262.
HARPER R. M. and GORDON W. E.	1980	*Radio Sci.* **15,** 195.
KATO S., OGAWA T., TSUDA T., SATO T., KIMURA I. and FUKAO S.	1984	*Radio Sci.* **19,** 1475.
LARSEN M. F. and RÖTTGER J.	1982	*Bull. Am. met. Soc.* **63,** 996.
RASTOGI P. K. and RÖTTGER J.	1982	*J. atmos. terr. Phys.* **44,** 461.
RÖTTGER J.	1980	*Pure appl. Geophys.* **118,** 494.
RÖTTGER J.	1984	*Handbook for MAP* **13,** 187.
RÖTTGER J. and LIU C. H.	1978	*Geophys. Res. Lett.* **5,** 357.
RÖTTGER J. and SCHMIDT G.	1979	*IEEE Trans. Geosci. Electron.* **GE-17,** 182.
RÖTTGER J., RASTOGI P. K. and WOODMAN R. F.	1979	*Geophys. Res. Lett.* **6,** 617.
SATO T. and WOODMAN R. F.	1982	*J. atmos. Sci.* **39,** 2546.
SATO T., TSUDA T., KATO S., MORIMOTO S., FUKAO S. and KIMURA I.	1985	*Radio Sci.* **20,** 1452.
TSUDA T., YAMAMOTO M., SATO T., KATO S. and FUKAO S.	1985	*Radio Sci.* **20,** 1241.
WAKASUGI K., FUKAO S., KATO S., MIZUTANI A. and MATSUO M.	1985	*Radio Sci.* **20,** 1233.
WAKASUGI K., MIZUTANI A., MATSUO M., FUKAO S. and KATO S.	1986	*J. atmos. oceanic Tech.* **3** (in press).
WAND R. H., RASTOGI P. K., WATKINS B. J. and LORIOT G. B.	1983	*J. geophys. Res.* **88,** 3851.
WOODMAN R. F.	1980a	*Radio Sci.* **15,** 417.
WOODMAN R. F.	1980b	*Radio Sci.* **15,** 423.

Reference is also made to the following unpublished material:

RÖTTGER J.	1985	Private communication.